Environmental Microbiology (2007) **9**(1), 93–106 doi:10.1111/j.1462-2920.2006.01119.x

Microbial diversity and dynamics in multi- and single-compartment anaerobic bioreactors processing sulfate-rich waste streams

Aurelio M. Briones,[1] Becky J. Daugherty,[1] Largus T. Angenent,[2] Kent D. Rausch,[3] Mike E. Tumbleson[3] and Lutgarde Raskin[1]*

[1]*Department of Civil and Environmental Engineering, University of Illinois at Urbana-Champaign, Urbana, IL 61801, USA.*

[2]*Department of Chemical Engineering and Environmental Engineering Science Program, Washington University in St Louis, St Louis, MO 63130, USA.*

[3]*Department of Agricultural and Biological Engineering, University of Illinois at Urbana-Champaign, Urbana, IL 61801, USA.*

Summary

We investigated bacterial and archaeal community structures and population dynamics in two anaerobic bioreactors processing a carbohydrate- and sulfate-rich synthetic wastewater. A five-compartment anaerobic migrating blanket reactor (AMBR) was designed to promote biomass and substrate staging, which partially separates the processes of methanogenesis and sulfidogenesis in the middle and outer compartment(s) respectively. The second reactor was a conventional, single-compartment upflow anaerobic sludge blanket (UASB) reactor. Both reactors, which were seeded with the same inoculum, performed well when the influent chemical oxygen demand (COD)/SO_4^{2-} mass ratio was 24.4. The AMBR performed worse than the UASB reactor when the influent COD/SO_4^{2-} mass ratio was decreased to 5.0 by raising the sulfate load. Terminal restriction fragment length polymorphism analyses of bacterial 16S rRNA genes showed that the increase in sulfate load had a greater impact on bacterial diversity and community structure for the five AMBR compartments than for the UASB reactor. Moreover, bacterial community profiles across AMBR compartments became more similar through time, indicating a converging, rather than a staged community. While similar populations were abundant in both reactors at the beginning of the experiment, fermenting bacteria (clostridia, streptococci), and sulfate-reducing bacteria became more abundant in the AMBR, after shifting to a higher sulfate load, while a novel *Thermotogales*-like population eventually became predominant in the UASB reactor. A similar shift in the community structure of the hydrogenotrophic methanogens in the AMBR occurred: representatives of the *Methanobacteriaceae* out-competed the *Methanospirillaceae* after increasing the sulfate load in the AMBR, while the archaeal community structure was maintained in the UASB.

Received 15 June, 2005; accepted 21 June, 2006. *For correspondence. E-mail raskin@umich.edu; Tel. (+1) 734 647 6920; Fax (+1) 734 763 2275.

Introduction

Anaerobic digestion is commonly employed to treat industrial waste streams of varying compositions and organic matter content. Among the various designs and configurations of anaerobic bioreactors, the most widely used is the upflow anaerobic sludge blanket (UASB) reactor (Franklin, 2001), which is a single-compartment reactor that relies on granulation to retain its biomass and can be operated at high organic and hydraulic loading rates (Lettinga *et al*., 1980). The UASB reactor configuration, however, often encounters problems such as bulking (Angenent and Sung, 2001) and suppression of methanogenesis (Yamaguchi *et al*., 1999) when treating wastewaters rich in carbohydrates and sulfate respectively. Under these conditions, a subtle balance between the competing processes of sulfidogenesis and methanogenesis is necessary to achieve complete removal of sulfate and organic matter. With the current level of understanding (reviewed in Colleran *et al*., 1995; Speece, 1996; Lens *et al*., 1998) it remains difficult to predict the process outcome for a given set of operating conditions.

In terms of the balance between organic matter (expressed as chemical oxygen demand, COD) and sulfate, the theoretical COD/SO_4^{2-} mass ratio needed to achieve complete removal of organic matter is 0.67, assuming eight electrons are transferred per molecule of sulfate (Lens *et al*., 1998). In practice, however, complete removal of organic matter requires a higher COD/SO_4^{2-}

mass ratio, in order to accommodate both sulfidogenesis and methanogenesis. In general, low and high COD/SO_4^{2-} mass ratios should favour sulfidogenesis and methanogenesis respectively. However, values reported in the literature for COD/SO_4^{2-} mass ratios vary considerably. Values favouring methanogenesis range from 6.0 or higher (Mizuno *et al*., 1994) to 8.0 or higher (Choi and Rim, 1991), while sulfidogenesis may be favoured at mass ratios of less than 5.0 (Choi and Rim, 1991; Annachhatre and Suktrakoolvait, 2001) or 1.5 or less (Mizuno *et al*., 1994). Given the uncertainty associated with process outcomes under sulfate-rich methanogenic conditions, new reactor designs provided an alternative option to improve anaerobic treatment.

Compartmentalized, anaerobic bioreactors may have advantages compared with single-compartment systems such as UASB reactors when treating wastewaters with high COD and sulfate content. In compartmentalized bioreactors, the initial compartments selectively promote fermentation and sulfidogenesis, leaving the inner compartment(s) predominantly methanogenic (Barber and Stuckey, 1999; Angenent and Sung, 2001; Angenent *et al*., 2002a). A recently developed bioreactor, designated as the anaerobic migrating blanket reactor (AMBR), provides this compartmentalized configuration (Angenent and Sung, 2001). This system consists of multiple (at least three) compartments, horizontally connected by small openings through which water and biomass are allowed to flow. This configuration creates a substrate gradient in the direction of flow, and promotes biomass staging, i.e. the partial separation between fermentative/sulfidogenic and methanogenic activities. To prevent biomass accumulation in the final compartment, the flow is reversed at regular time intervals. The AMBR has proven to provide for stable operation during high organic shock loads (Angenent *et al*., 2002b). However, the performance of an AMBR under sulfate-rich conditions has not been evaluated.

Although the processes that occur during anaerobic digestion (hydrolysis, fermentation, acetogenesis, methanogenesis, sulfidogenesis) are well described, the relationships among microbial community composition, diversity, and dynamics, and reactor performance are not well understood. Several studies have related population dynamics to reactor performance; however, most of these studies have targeted specific populations only, including methanogens (Raskin *et al*., 1994; Griffin *et al*., 1998; Angenent *et al*., 2002c), sulfate-reducing bacteria (SRB), and syntrophic bacteria (Hansen *et al*., 1999; McMahon *et al*., 2001; 2004; Zheng *et al*., 2006). A few studies have reported on bacterial diversity in anaerobic bioreactors (Godon *et al*., 1997; Sekiguchi *et al*., 1998), although these did not provide information on population dynamics and succession events.

This study was conducted to compare performances of multi- and single-compartment anaerobic bioreactors treating a carbohydrate- and sulfate-rich wastewater. A five-compartment AMBR and a conventional UASB reactor were selected to accomplish this objective. We monitored changes in diversity and dynamics of abundant groups of bacteria and archaea that developed in these anaerobic bioreactors and related these microbial findings to the contrasting performances of the two bioreactors.

Results

Reactor performance

The operational time for both reactors was divided into two periods with different influent sulfate concentrations. During Period 1 (days 0–99), the COD/SO_4^{2-} mass ratio in the influent was maintained at 24.4 (7000 mg l^{-1} COD; 287 mg l^{-1} SO_4^{2-}), while during Period 2 (days 100–149), the influent sulfate concentration was increased to reach a COD/SO_4^{2-} mass ratio of 5.0 (1400 mg l^{-1} SO_4^{2-}). The volumetric loading rate (VLR) was increased from the startup VLR of approximately 5 g COD l^{-1} day^{-1} to 10 g COD l^{-1} day^{-1} on day 10 and to approximately 15 g COD l^{-1} day^{-1} on day 75 (Fig. 1A). Before day 15, the total volatile fatty acids (VFA) concentration in the effluent of both reactors was less than 500 mg l^{-1} as acetate (Fig. 1D). The first increase in VLR resulted in an increase in VFA concentrations in the effluents of both reactors. Subsequently, VFA levels gradually decreased, but the levels remained higher for the AMBR (Fig. 1D). The second increase in VLR did not result in a substantial increase in VFA levels. By the end of Period 1, the AMBR and UASB reactor effluents contained VFAs at approximately 1000 and 450 mg l^{-1} as acetate respectively.

When the influent sulfate concentration was increased on day 100, VFA levels in the AMBR effluent began to increase soon thereafter and remained high for the rest of the operational period (Fig. 1D). Substantial VFA accumulation occurred in the UASB reactor only after 22 days into Period 2. Large fluctuations in effluent VFA concentrations were observed for both reactors between days 122 and 128, which were the result of an optimization attempt from days 119–121, during which the alkalinity of the feed solution was decreased by 25%. Eight days after the alkalinity was returned to the previous level, operational parameters returned to those observed prior to the unsuccessful optimization attempt.

During Period 1, soluble chemical oxygen demand (SCOD) removal in the AMBR and UASB reactor averaged 77% and 88% respectively, with coefficients of variation of 13% and 9% respectively (Fig. 1B). When the influent sulfate concentration was increased on day 100, an immediate decrease in SCOD removal was observed

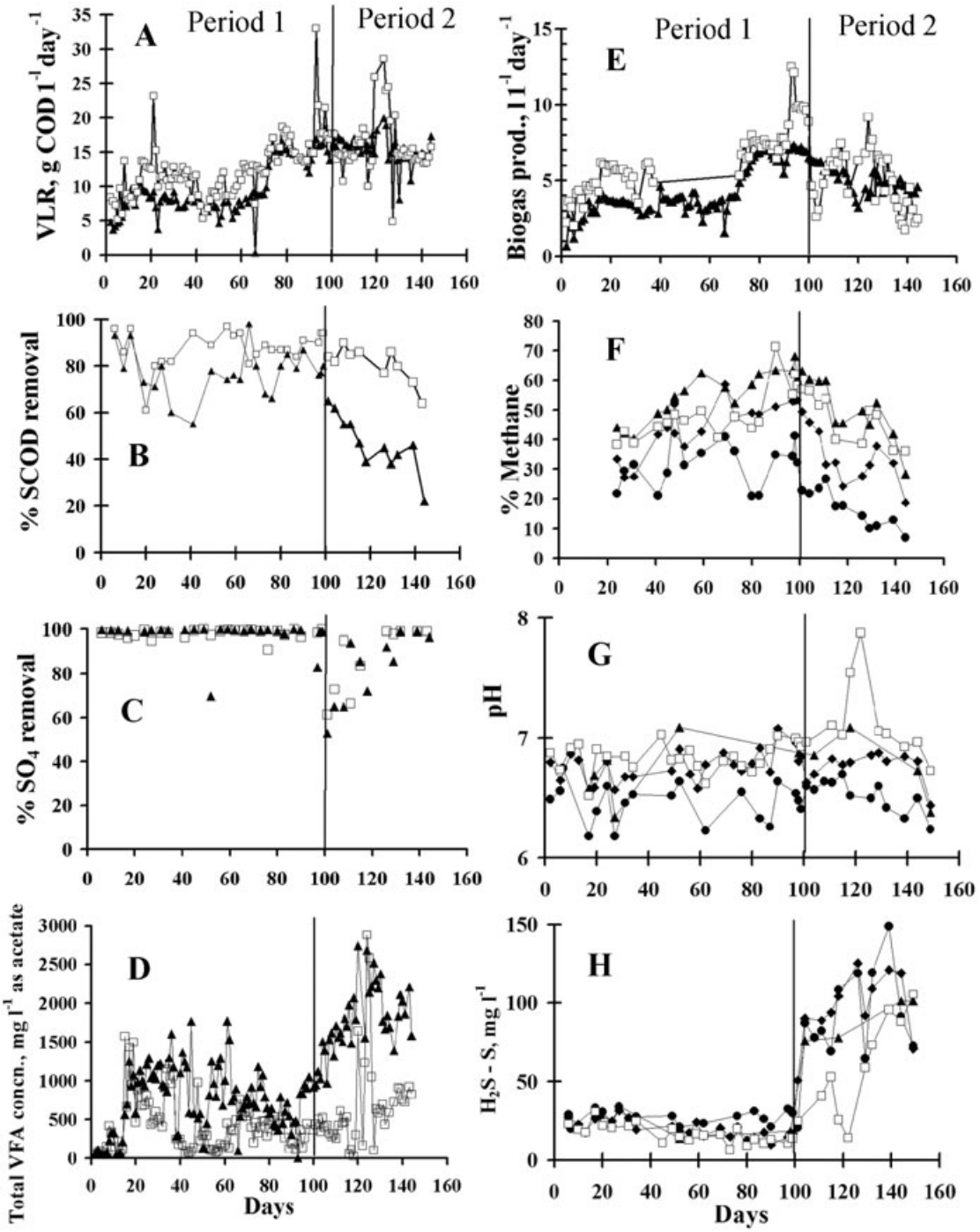

Fig. 1. Operational and performance data for AMBR and UASB reactor.
A. Volumetric loading rates (VLR).
B. Per cent SCOD removals.
C. Per cent sulfate removal.
D. Effluent total VFA concentrations.
E. Biogas production rates; rates for the AMBR represent the cumulative production by each compartment.
F. Per cent methane measured in the biogas of each compartment of the AMBR and UASB.
G. pH in outer and middle AMBR compartments and in UASB reactor.
H. H_2S concentrations expressed as S in the outer and middle AMBR compartments and UASB effluent.
In A, B, C, D and E, ▲ denotes AMBR and □ denotes UASB. In F, G and H, □ indicates UASB; ● indicates Compartment 1; ▲ indicates Compartment 3; and ◆ indicates Compartment 5.

in the AMBR (from 80% to 65% in 2 days), which corresponded to the rapid increase in effluent VFA levels. Soluble chemical oxygen demand removal continued to decrease throughout Period 2, and by day 144, SCOD removal in the AMBR had reached a minimum of 20%. The UASB reactor maintained an average SCOD removal of 84% for 29 days after raising the SO_4^{2-} level. After the temporary decrease in influent alkalinity, SCOD removal tapered off to 64% by day 144.

Throughout the experiment, methane levels in the headspaces of compartments 1 and 3 of the AMBR were generally lowest and highest respectively (Fig. 1F). The methane levels in the outermost (compartments 1 and 5) and middle (compartment 3) AMBR compartments averaged 43% and 60%, respectively, by the end of Period 1. By the end of Period 2, the methane levels in outermost and innermost compartments averaged 13% and 28% respectively. Changes in methane levels in the biogas collected from the UASB reactor ranged from 40% to 70% during Period 1, achieving a level of 60% at the end of this period. After the increase in sulfate concentration, methane in the biogas declined to about 36% near the end of Period 2. Total biogas production rates for all AMBR compartments combined and for the UASB reactor are shown in Fig. 1E; the UASB reactor outperformed the AMBR during most of the operational period. Comparisons of biogas production rates in individual compartments of the AMBR showed consistently higher biogas production rates in the outermost compartments and the lowest biogas production rates in the middle compartment (data not shown).

Sulfate removal efficiencies were similar for both reactors (Fig. 1C). During Period 1, the sulfate removal efficiency was approximately 97% in both reactors. After changing the COD/SO_4^{2-} mass ratio to 5, the sulfate removal efficiency first decreased to around 50%, then increased to values similar to those observed during Period 1. There were no obvious differences in trends for the concentration of total sulfides in selected AMBR compartments and in the UASB reactor effluent (data not shown). However, due to the higher pH in the UASB reactor during Period 2 (Fig. 1G), H_2S levels in the UASB reactor were generally lower (Fig. 1H). The exception to this observation occurred at the end of Period 2, when H_2S levels in the UASB increased above 100 mg H_2S-S l^{-1}, while levels in compartments 1 and 5 of the AMBR decreased to approximately 70 mg l^{-1}. H_2S toxicity may have been significant in the AMBR as early as 18 days into Period 2, when levels reached values higher than 100 mg H_2S-S l^{-1} in compartments 1 and 5.

Both reactors were inoculated with biomass from a UASB reactor that treated brewery wastewater. Inoculum granules were disintegrated before seeding the reactors. The biomass that developed within the UASB reactor consisted of large, dark-grey granules that formed within the first 2 weeks of operation. These granules were maintained for the entire operational period. Smaller, black granules were formed during the first week of operation in the AMBR. However, these granules were not maintained and were gradually replaced starting from the second week of operation by grey, fluffy biomass, which was eventually washed out by increasing the mixing frequency in the compartments. By the start of Period 2, the predominant biomass type in the AMBR consisted of flocs rather than granules.

Archaeal population dynamics

Clones were generated from PCR products obtained from biomass samples of the UASB reactor and from pooled PCR products from reactions performed with biomass samples collected from all compartments of the AMBR for days 2 and 127 of reactor operation. For each reactor and sample date, 48 clones were screened. Amplified ribosomal DNA restriction analysis (ARDRA) of archaeal clone libraries yielded 11 unique 16S rRNA gene restriction types based on HaeIII digestion. Sequencing of representative clones revealed that all ARDRA types were affiliated with species belonging to the genera *Methanosaeta*, *Methanospirillum* or *Methanobacterium*. The distribution of methanogen-affiliated 16S rRNA sequences were similar in both reactors at the beginning of the experiment (day 2) (Fig. 2B). *Methanosaeta*-related sequences were most frequently retrieved, representing 63% of clones in both reactors on day 2. *Methanobacterium*-related sequences represented 33% and 29% of the clones in the AMBR and UASB reactor respectively, and sequences affiliated with *Methanospirillum* represented 4% and 8% of the clones in the AMBR and UASB reactor respectively.

After 127 days of operation, the sequences retrieved from the AMBR clone libraries suggested a shift in the distribution of hydrogenotrophic methanogens: *Methanospirillum*-related sequences had increased from 4% to 44% and *Methanobacterium*-related sequences had decreased from 33% to 4%. *Methanosaeta*-related sequences remained predominant. On the other hand, the relative distribution of methanogens in the UASB remained similar, although the methanogenic populations either increased (*Methanosaeta*) or decreased (*Methanobacterium* and *Methanospirillum*) resulting in a less even distribution (Fig. 2B).

The terminal restriction fragment length polymorphism (T-RFLP) data presented in Fig. 2A confirm the trends detected in the clone libraries, although comparisons of the absolute quantities between the two methods showed disagreement. This is to be expected, because both methods are semiquantitative, and serve only to detect trends. The availability of T-RFLP data through the opera-

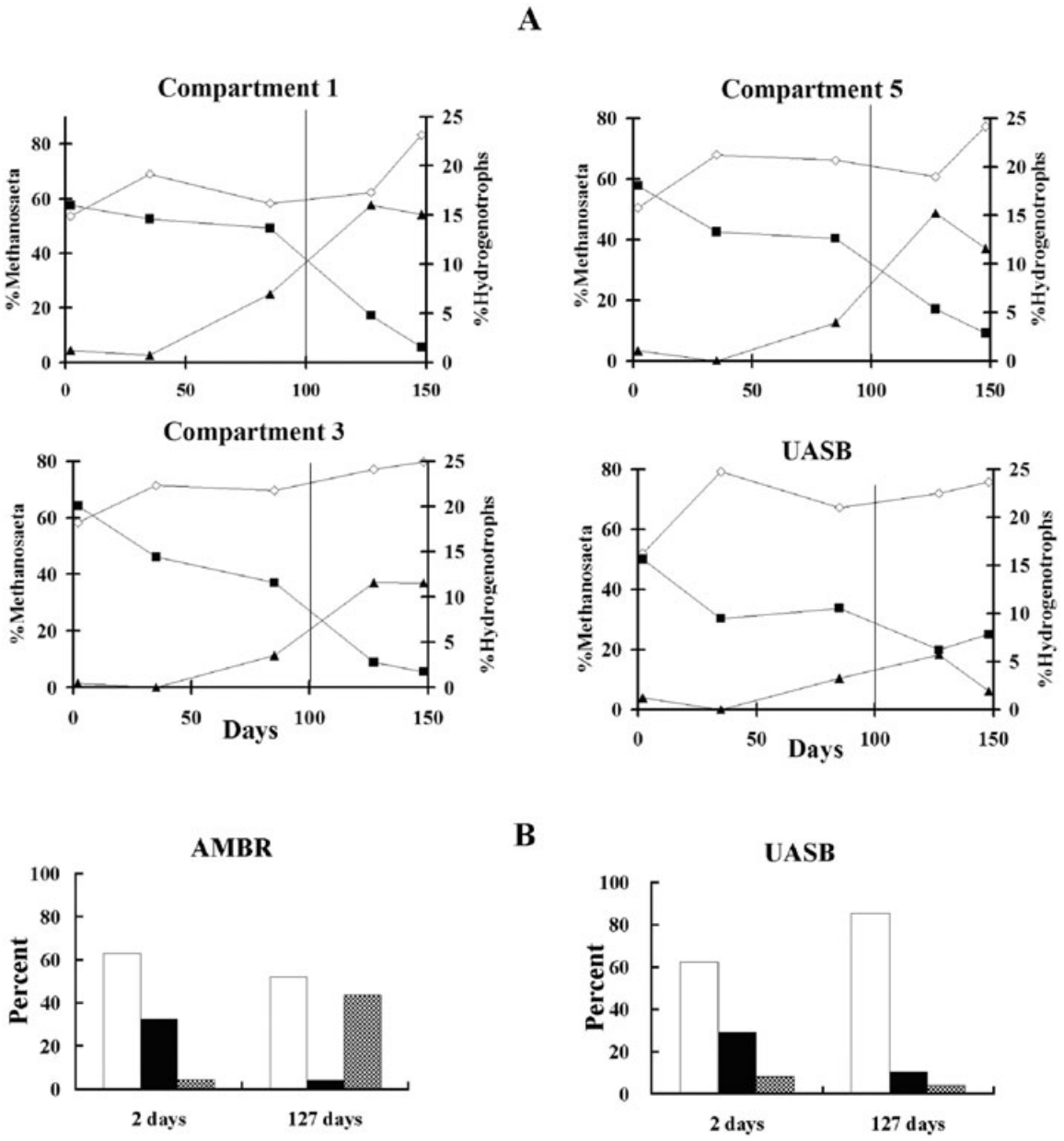

Fig. 2. Dynamics of three main groups of archaea detected in this study determined by (A) T-RFLP and (B) clone library analysis.
A. ◇, *Methanosaeta*; ■, *Methanobacterium*; ▲, *Methanospirillum*.
B. □, *Methanosaeta*; ■, *Methanobacterium*; ▩, *Methanospirillum*.

tional period allowed us to monitor changes in community structure over time. Differences in trends and community profiles among AMBR compartments were minimal. The temporal profiles suggest that the transition from *Methanobacterium* to *Methanospirillum* prominence took place after the change in sulfate loading (Fig. 2A).

Dynamics of abundant bacterial populations

The dynamics of the abundant bacterial populations within the AMBR and UASB reactor as determined by T-RFLP analysis are presented in Fig. 3. The abundant populations were defined as those whose total peak heights of their corresponding terminal restriction fragments (T-RFs) constituted at least 20% of the cumulative T-RF peak heights on at least one sampling date. Representatives of the clostridia were most frequently encountered in the clone libraries, and to simplify the analysis, the two most consistently detected populations using both T-RFLP and cloning were included in Fig. 3. This approach resulted in the monitoring of 10 unique populations over the entire experiment. These populations

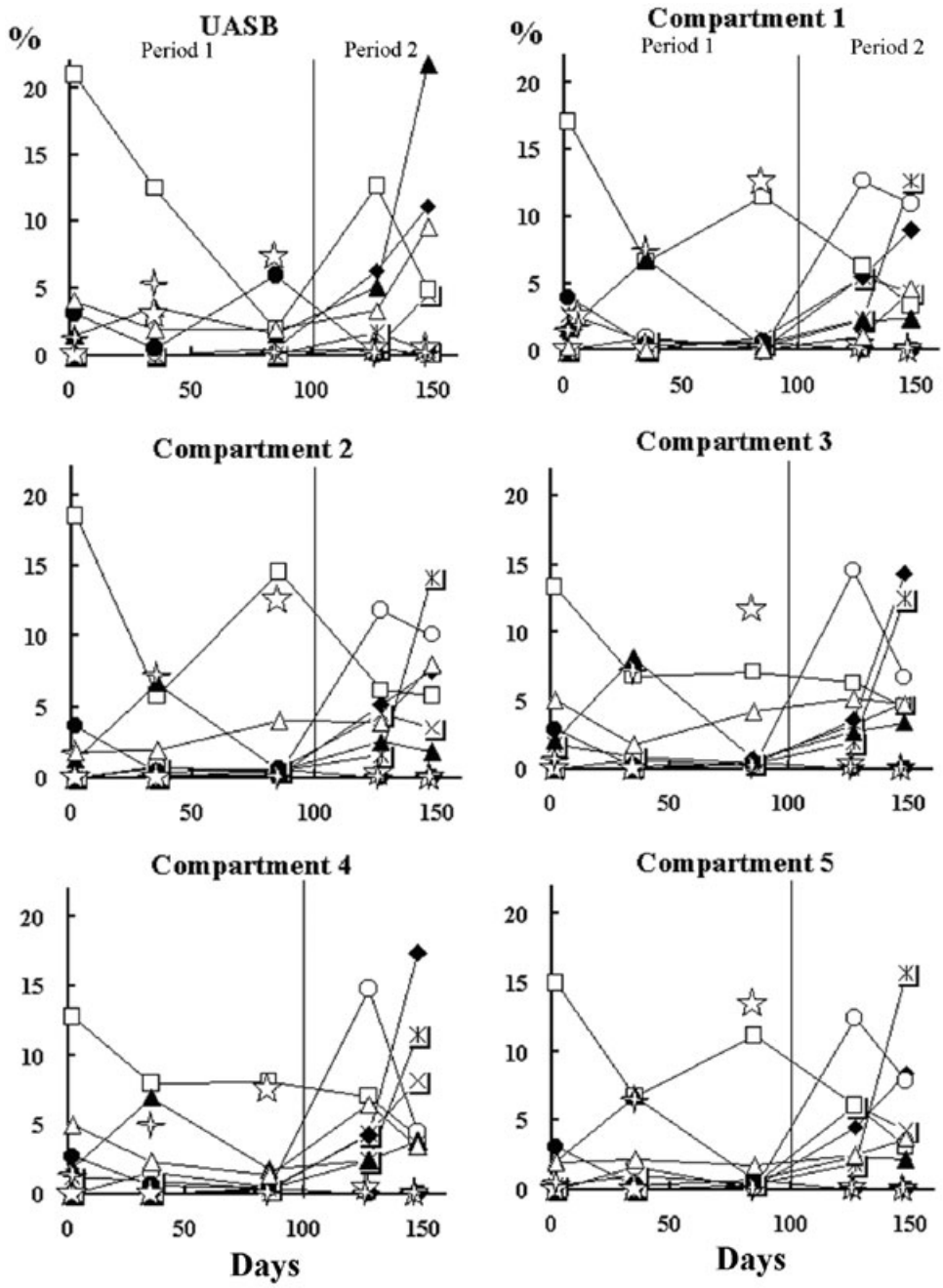

Fig. 3. Dynamics of bacterial populations in AMBR and UASB as determined by normalized T-RF peak height comparisons during T-RFLP analysis. The numbers after the names refer to T-RF sizes. ▲, *Thermotogales*-297; ○, *Clostridium*-271; ●, *Clostridium*-214; □, *Bacteroides*-261; ◆, *Desulfovibrio*-201; △, *Bacteroides*-37; ∗, *Streptococci*-265; ×, *Spirochaeta*-67. The stars represent unidentified T-RF peaks.

constituted 20–53% of the entire bacterial community during the five sampling periods. The populations were identified by BLAST searches of sequences obtained for the corresponding clones that yielded T-RFs with the same length as the T-RFs in the environmental PCR digests. Only eight of the 10 abundant populations could be identified based on clone sequence information. The unidentified populations (represented by stars in Fig. 3), which were present on sampling dates for which no clone libraries were constructed, were only transiently abundant in at least one compartment.

On day 2 of the operational period, a *Bacteroides*-like population (*Bacteroides*-261; based on closest affiliation by BLAST searches; the number at the end refers to the

T-RF size) was the most abundant population in all AMBR compartments and the UASB reactor, constituting 13–21% of the bacterial community. Between days 2 and 35, the relative abundance of the *Bacteroides*-261 population decreased, but it remained an abundant population in the AMBR compartments on day 35. Between days 35 and 127, the relative abundance of the *Bacteroides*-261 population either remained relatively constant (compartments 3 and 4) or fluctuated up and down (compartments 1, 2 and 5). By day 127, a *Clostridium* population designated as *Clostridium*-271 succeeded the *Bacteroides*-261 population as the predominant population in all AMBR compartments.

By day 148, different populations had gained prominence in different compartments of the AMBR; these constituted either a *Streptococcus*-like population (compartments 1, 2 and 5) or a *Desulfovibrio*-like population (compartments 3 and 4). Other populations that were detected at levels greater than 5% in at least one AMBR compartment on day 148 were: *Clostridium*-271, two *Bacteroides*-like populations (*Bacteroides*-261 and *Bacteroides*-37), and a *Spirochaeta*-like population (*Spirochaeta*-67). Most of the succession events were observed after the increase in influent sulfate levels (i.e. during Period 2).

The trends observed for the UASB reactor were similar to those described for the AMBR, except for two notable exceptions. First, the *Bacteroides*-261 population, which was predominant during the initial period of operation, was able to recover from a decrease in relative abundance (day 85) and again became the most abundant population on day 127. In contrast, *Clostridium*-271 had succeeded the *Bacteroides*-like population as the predominant population on day 127 in the AMBR. Second, a *Thermotogales*-like population became abundant in the UASB reactor after day 127. On day 148, this population became predominant, constituting 22% of the bacterial community. Phylogenetic analysis shows that this population, coded as AUTHM297 in Fig. 4, is affiliated with high bootstrap support to the *Geotoga-Petrotoga* lineage of the *Thermotogales*. While there was a moderately high level of bootstrap support to affiliate AUTHM297 with the genus *Petrotoga*, the sequence similarity to representative sequences within this genus was only 83%, indicating that the sequence generated in this study is novel.

Bacterial diversity

While the previous section focused only on abundant populations, the overall bacterial diversity was assessed by comparing three diversity metrics: the number of T-RFs present (richness, S), the evenness of T-RF abundance (evenness or equitability, *e*), and the Shannon–Weaver diversity index (H), which is a statistic that takes into account both species richness and the evenness of species distribution to estimate the level of entropy or diversity in a system. H tends to increase when either richness or evenness increases. Bootstrap resampling of diversity metrics among the different AMBR compartments failed to detect significant differences in diversity levels between compartments (data not shown) during all sampling dates. Therefore, the AMBR data in Table 1 show the values of H, S and *e* averaged among the different compartments, while the UASB data were averaged across two replicates. The maximal decrease from initial diversity values in both reactors occurred at the end of Period 2. In the AMBR, H decreased by an average of 1.1 from initial values, corresponding to an average of 71% decrease in S. In the UASB, H decreased by only 0.4, although S decreased by around 55%. In addition to the smaller change in S, the minimal change in H in the UASB could also be attributed to a comparatively large increase in *e* (from 0.83 to 0.92).

Analysis of bacterial community structure based on T-RF profiles

Results of cluster analysis on T-RF profiles derived from single samples collected on days 2 and 148 are shown in Fig. 5A and B respectively. On day 2, the branch lengths (represented by semi-partial r^2 values between clusters) joining each cluster ranged from 0.10 to 0.33. At this time, the bacterial community in the UASB reactor was sufficiently similar to the communities in the AMBR compartments (because they were derived from the same inoculum source) to cluster together with one of the communities in the AMBR compartments (compartment 2 in the example in Fig. 5A). However, by day 148, the UASB reactor community had diverged greatly from the communities in the AMBR compartments (branch length between AMBR cluster and UASB reactor cluster, 0.83). The divergence of the UASB reactor community was apparent by day 35, when it had already formed a unique cluster separated from the AMBR cluster (data not shown). On the other hand, the distances between clusters of AMBR compartments generally decreased through time (average of 0.20–0.05 from days 2–148). While all trees consistently showed the divergence of AMBR and UASB communities through time, the topology of branches between AMBR compartments did not show any consistent relationships that could be supported by replicate samples. Furthermore, cluster analysis did not detect any consistent affiliations (or differences) among AMBR compartments that were stably maintained through time.

The T-RF profiles from three sampling dates (days 2, 85 and 148) were summarized using correspondence

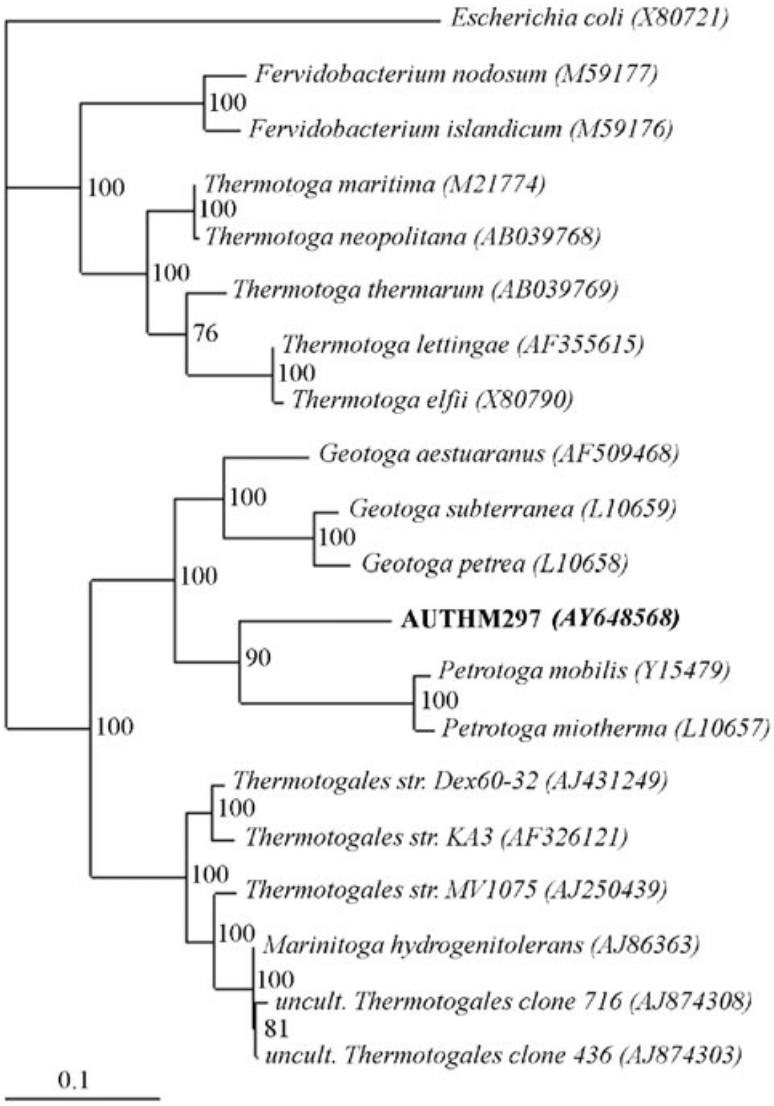

Fig. 4. Phylogenetic tree showing the affiliation of clone AUTHM297 to other known lineages within the *Thermotogales*. The tree was generated using the maximum likelihood algorithm DNAML in Phylip 3.6. Bootstrap values greater than 50% are presented. The scale bar represents 0.10 changes per nucleotide.

analysis, an ordination method that plots information on taxa (T-RFs) and samples (compartments) in a two-dimensional graph whose axes account for a fraction of the total variability. Samples with similar community structures are clustered together in the scatter diagram. Figure 5C shows the scatter plot of the different AMBR compartments and the UASB reactor. The samples collected from the three sampling dates formed three main clusters. The data points from day 2 samples (cluster III) did not show a clear separation between the UASB

Table 1. Changes in bacterial diversity through time based on T-RFLP analysis.

		Days after startup				
		Period 1			Period 2	
Reactor		2	35	85	127	148
AMBR	OTU richness, S	84	70	110	95	24
	Shannon–Weaver diversity index, H	3.90	3.86	3.85	3.79	2.80
	Evenness, *e*	0.88	0.91	0.82	0.83	0.88
UASB	OTU richness, S	76	74	89	97	34
	Shannon–Weaver diversity index, H	3.59	3.86	3.91	3.82	3.19
	Evenness, *e*	0.83	0.90	0.87	0.84	0.91

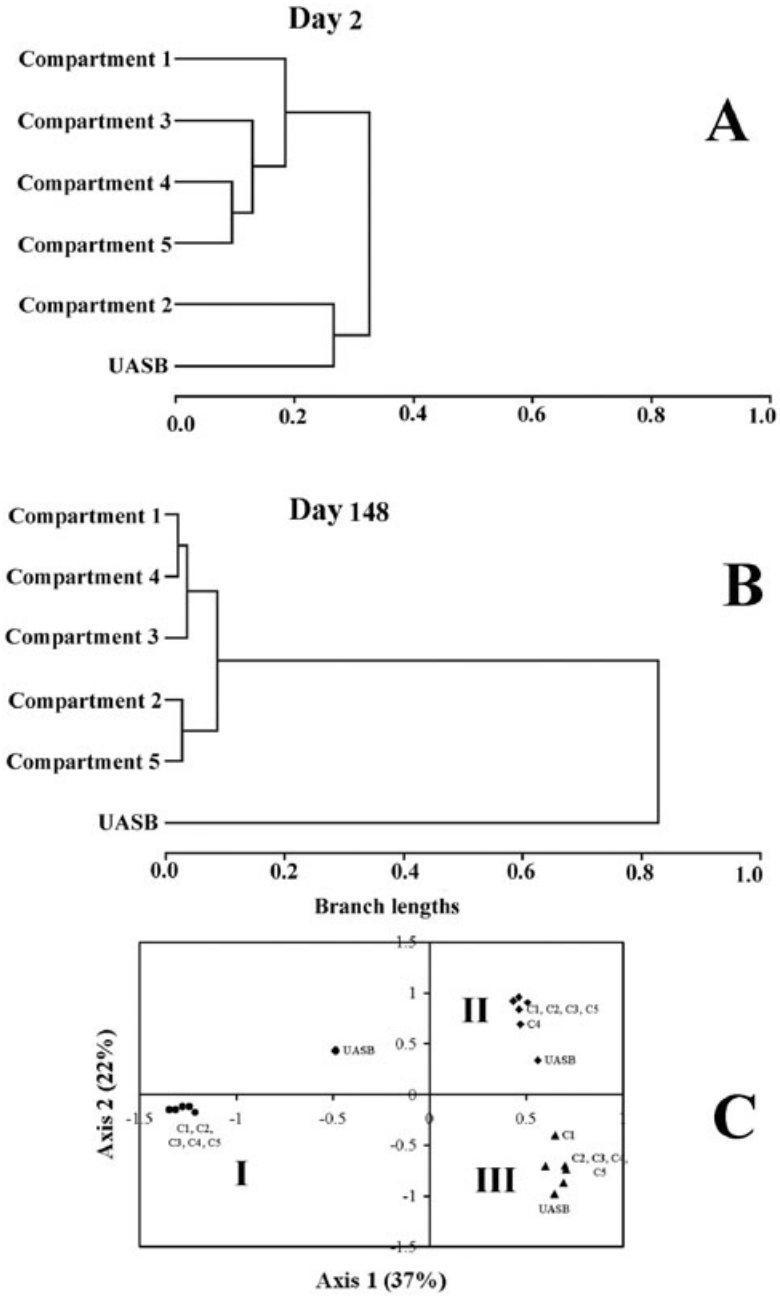

Fig. 5. Comparison of T-RF profiles by cluster analysis. (A) and (B) illustrate results of analysis of single samples collected on days 2 and 148. (C) shows a correspondence analysis of T-RFLP data for UASB reactor and each AMBR compartment from samples collected on day 2 (▲), day 85 (◆) and day 148 (●).

reactor and AMBR compartments. As the experiment progressed (day 85), the data points from the AMBR clustered closer together, and the UASB reactor data could be distinguished along Axis 2 (cluster II). By the end of the experiment, the community structure in the AMBR compartments had become highly similar, while the UASB reactor community clearly had separated (cluster I). The AMBR cluster for day 148 (cluster 1) was more clearly separated from either clusters II or III compared with the UASB reactor community, suggesting that the divergence between the UASB reactor and AMBR on day 148 was due primarily to the changing community structures in the AMBR compartments.

Discussion

The AMBR was developed to promote biomass staging (variable community structures in different compartments) and substrate staging (variable functions and activities in different compartments), and in particular, to promote the partial separation of fermentative and methanogenic processes (Angenent and Sung, 2001). The anticipated

selection of methanogens in the middle of the AMBR was supported by consistently higher levels of methane in the biogas of compartment 3 compared with the other compartments (Fig. 1D). However, in contrast to expectations, methane production in the outer compartments was still quite substantial and methanogenic populations in these compartments were similar to those in the middle compartment. Similarly, H_2S production was not confined to the outer compartments and a *Desulfovibrio*-like population became abundant in the middle compartments (compartments 3 and 4) during Period 2. Fermentative populations, such as clostridia and streptococci, were abundant in the outer compartments (compartments 1, 2 and 5), which was according to expectations. These results suggest that, while some degree of staging may have been achieved in the AMBR, sulfate reducers and methanogens remained competitive in the middle and outer compartments respectively.

Although the microbial community structures and diversities of the AMBR and UASB reactor were similar at the start of the experiment, the UASB reactor exhibited more stable performance and changed less in terms of diversity and community structure compared with the AMBR after being challenged with a high sulfate load. The UASB reactor outperformed the AMBR in terms of SCOD removal, which became more evident after lowering the COD/SO_4^{2-} mass ratio from 24.4 to 5.0 (Fig. 2B). The contrast in performance was supported by lower VFA accumulation and higher biogas production rates in the UASB reactor. The poor performance of the AMBR compared with the UASB reactor was surprising, because its staged design was expected to cope with a carbohydrate- and sulfate-rich influent better. However, the degree of biomass and substrate staging achieved in the AMBR was minimal. Sulfate-reducing bacteria were able to remain abundant in the middle compartments, methanogens continued to be active in the outer compartments, and the overall microbial community structure across all AMBR compartments converged.

The contrasting performances of the two bioreactors may be related to the contrasting dynamics of a population that became predominant in the UASB. The order *Thermotogales* is comprised of members that are thermophilic or hyperthermophilic and represent an early divergence in the bacterial line of descent (Winker and Woese, 1991). All of the characterized members of the order are obligate anaerobes, fermentative, and capable of reducing elemental sulfur and/or thiosulfate (Stetter *et al*., 1990; Ravot *et al*., 1995). Most cultured representatives have been isolated from natural ecosystems such as deep-sea vents, hot springs and petroleum reservoirs. Balk and colleagues (2002) described the isolation and characterization of a member of this group (*Thermotoga lettingae* strain TMO^T) from a thermophilic, sulfate-reducing bioreactor. Interestingly, aside from being able to ferment a wide variety of complex substrates, strain TMO^T is also able to utilize fermentation products such as acetate when suitable electron acceptors, such as elemental sulfur or thiosulfate, are available, or in the presence of a syntrophic partner, such as the methanogen *Methanothermobacter thermoautotrophicus* ΔH (Balk *et al*., 2002).

The *Thermotogales*-like population detected in our study grew under mesophilic conditions (35.5°C) and was affiliated with the *Petrotoga-Geotoga* lineage, based on 16S rRNA gene similarity. Although it is not closely related to strain TMO^T, based on known physiological characteristics of the *Thermotogales*, it is likely that AUTHM297 is a fermenter and capable of utilizing elemental sulfur and/or thiosulfate as electron acceptors to form H_2S. The higher tolerance to H_2S by this group of bacteria (Stetter *et al*., 1990) was consistent with the higher efficiency of SCOD removal in the UASB reactor during Period 2, because H_2S levels reached values (100 mg H_2S-S l^{-1} or more) that would have been inhibitory to COD removal by other populations (Yamaguchi *et al*., 1999).

Although the *Thermotogales*-like population was also detected in the AMBR, it did not become abundant within this bioreactor. A possible hypothesis for the contrasting dynamics of this population in the two bioreactors could be related to the dynamics of the hydrogenotrophic methanogens detected in our systems. At least one member of *Methanobacteriaceae* can serve as a syntrophic partner for a *Thermotogales* species (Balk *et al*., 2002). If a similar syntrophic partnership was occurring in our systems, then the decline of the methanobacteria and increase of methanospirilla in the AMBR may partly explain the lack of competitiveness of AUTHM297 in this bioreactor.

The decreasing methane and increasing sulfide production in both bioreactors during Period 2 would suggest the emergence of a sulfur-driven metabolism responsible for organic matter breakdown. Such a shift has been previously reported in UASB reactors treating sulfate-containing wastewater (Harada *et al*., 1994; Yamaguchi *et al*., 1999). In these reports, however, the dominant metabolic pathway was mediated by SRB. The abundance of a *Thermotogales*-like population that does not require sulfate in a mesophilic reactor treating sulfate-rich wastewater is a new finding, and further investigations will be required to determine how important this type of sulfur metabolism is in anaerobic bioreactors.

While it is tempting to ascribe the performance of the reactors to the abundant bacterial and archaeal populations presented here, other factors likely contributed to reactor performance. These include interspecies competition and syntrophic interactions as well as contrasting system perturbations due to differences in the reactors' mixing regime. These possibilities require further investigation. While this retrospective microbial commu-

nity characterization has provided useful information to help explain bioreactor performance, it would have been more fruitful to perform microbiological analyses concurrently with bioreactor operation and to use this information to modify operating conditions. High throughput and rapid methods for quantitative population studies are necessary to make this a reality.

Experimental procedures

Configuration and operating conditions of reactors

Details of the design and construction of the AMBR were reported previously (Angenent and Sung, 2001; Angenent *et al*., 2002a). A reactor containing five 4 l compartments (Angenent *et al*., 2002c) was fed using four separate peristaltic pumps (Peristaltic, Masterflex, Barrington, IL). To achieve four flow reversals per day, the initial compartment was fed for 4 h, followed by 2 h of feeding into the adjacent compartment. The flow was then reversed using the same feeding regime in the opposite direction. The middle compartment was never fed directly. Effluent flowed from the reactor by gravity while two automatic ball valves (True blue electric actuator model EBV-6, Plast-o-matic valves, Cedar Grove, NJ) opened and closed the two effluent ports. Baffles present at each of the effluent ports prevented large amounts of biomass from leaving with the effluent.

The flow reversal of four times per day was maintained up to 128 days, after which the flow reversal scheme was reduced to twice per day (days 129–144) and then to once a day (days 145–149). These changes were performed to reduce pH (primarily in the initial compartments) and enhance staging in the AMBR. For the same reasons, the alkalinity of the feed was decreased by 25% for 3 days (days 119–121).

Mixing in each compartment was achieved using mixers (Model 5vb, EMI, Clinton, CT) and impellers (Lightnin A-310 axial flow, Rochester, NY), which were used intermittently for 10 s every 10 min at a speed of 100 rpm. The mixing in the final compartment was set at 10 s every 10–30 min, depending on the level of biomass wastage desired.

The UASB reactor consisted of a glass cylinder with an inner diameter of 7.5 cm and a working volume of 4.9 l. The influent and recycle flow were introduced at the bottom of the reactor with an upflow velocity of 1 m h^{-1} using peristaltic pumps (Masterflex, Barrington, IL). The recycle flow rate was nine times the influent flow rate. Glass marbles (diameter 1 cm) were placed at the bottom of the reactor to ensure even flow distribution. An inverted funnel was placed at the top of the reactor to facilitate gas-liquid-solid separation.

The reactors were operated in a temperature control room set at 35.5°C; they were inoculated with granular biomass collected from a UASB reactor operated by the Anheuser Busch Brewery (St Louis, MO). Granules for both reactors were distributed within the AMBR compartments and crushed by operating the mixers at a speed > 200 rpm for 16 h. The initial mixed liquor volatile suspended solids concentration in both reactors was approximately 30 g l^{-1} and the initial VLR was approximately 5 g COD l^{-1} day^{-1}. The VLR was gradually increased until attaining the target VLR of 15 g COD l^{-1} day^{-1} (Fig. 1A). The target hydraulic retention time was 11 h. The solids retention times (SRTs) in the AMBR during Periods 1 and 2 averaged 60 and 83 days respectively. The SRTs for the corresponding periods for the UASB reactor averaged 43 and 15 days.

The reactors were fed with a solution containing (per litre) 7.7 g corn syrup (Clearsweet 43/43, Cargill, Cedar Rapids, IA), 4.2 g $NaHCO_3$, 521 mg (Period 1) or 2541 mg (Period 2) K_2SO_4, 79 mg Na_2SO_3, 187 mg NH_4Cl, 38 mg KNO_3, 28 mg K_2HPO_4, 22 mg $NaH_2PO_4{\cdot}H_2O$ and 42 mg yeast extract. In addition, 0.07 ml trace element solution was added per gram of COD. The trace element solution contained (per litre): 2 g $FeCl_2{\cdot}4H_2O$, 2 g $CoCl_2{\cdot}6H_2O$, 1 g EDTA, 0.5 g $MnCl_2{\cdot}4H_2O$, 0.142 g $NiCl_2{\cdot}6H_2O$, 0.123 g Na_2SeO_3, 13.6 mg $MgCl_2$, 90 mg $AlCl_3{\cdot}6H_2O$, 50 mg H_3BO_3, 50 mg $ZnCl_2$, 50 mg $(NH_4)_6Mo_{24}{\cdot}4H_2O$, 38 mg $CuCl_2{\cdot}2H_2O$, 1 ml 37.7% HCl and 0.2 g resazurin. After dilution of the concentrated nutrient stock, the pH of the influent was 7, and the COD was 7000 mg l^{-1}. The feed mixture was developed to simulate the composition of a wastewater from a corn wet-milling plant (Daugherty, 2002), while the trace element solution was modelled after Zehnder and colleagues (1980).

Analytical methods

Liquid and biogas samples from the effluent, individual compartments and compartment headspaces were collected at the midpoint of the time interval between two flow reversals, usually at the same time of the day from the AMBR, and effluent and biogas samples were collected from the UASB reactor. Liquid samples for chemical analyses were filtered through a 0.45 μm pore size membrane filter and stored at 4°C until further analysis. Samples for individual VFA analysis were acidified with 2 N H_2SO_4 and analysed for VFAs with a high performance liquid chromatography system (Waters 486, Milford, MA) equipped with a UV detector and an HPX-87H column (Bio-Rad, Hercules, CA). Measurements of total suspended solids, volatile suspended solids, total VFAs, pH, alkalinity, total and soluble COD and sulfide were conducted according to standard methods (Greenberg *et al*., 1992). Total sulfides were measured using the methylene blue spectrophotometric method (Greenberg *et al*., 1992), while aqueous H_2S was calculated based on the following equation (Speece, 1996): H_2S fraction $= 1/[1 + (K_1/10^{-pH}]$, where K_1 is the first ioinization constant of H_2S and is equal to $10^{-6.83}$ at 35°C.

Sulfate and sulfite were measured with a Dionex ion chromatograph (DX600, Sunnyvale, CA) equipped with a Dionex ED50 electrochemical detector and a Dionex AS11 column. Methane and hydrogen in the biogas were measured using a gas chromatograph (Perkin Elmer, Norwalk, CT) equipped with a GS-Q column (J and W Scientific, Folsom, CA) and a flame ionization detector (FID) maintained at 40°C and a reduction gas detector (RGD, Trace Analytical, Menlo Park, CA). Using He as carrier gas, a 10-port actuated valve (Valco Instruments, Houston, TX) enabled the sample flow to pass through the FID or the RGD to measure methane and hydrogen respectively.

DNA extraction, PCR and construction of clone libraries

Biomass was sampled from each compartment of the AMBR and from the UASB reactor (composite samples collected

through sampling ports placed at 10 cm intervals at the side of the UASB reactor were obtained), pelleted in 2 ml microcentrifuge tubes to achieve at least 100 mg of biomass (wet weight), and immediately frozen at −80°C. DNA was extracted using a combined detergent and bead beating procedure (UltraClean Soil DNA Kit, Mo Bio Laboratories, Carlsbad, CA) following the manufacturer's instructions. PCR targeting 16S rRNA genes of all bacteria was performed using primers 27f and 1392r (Lane, 1991). PCR mixtures (100 μl) contained: 10 μl Takara *Ex Taq* 10× PCR buffer (Takara Shuzo, Shiga, Japan), 1 mM $MgCl_2$, 200 μM of each dNTP, 0.1 μM primers, approximately 30 ng DNA template and 2.5 units of *Ex Taq* DNA polymerase. The reaction mixture was amplified using a thermal cycler (PTC-200, MJ Research, Reno, NV) programmed to run one denaturation step at 94°C for 2 min, followed by 30 cycles of denaturation at 94°C for 30 s, annealing at 50°C for 15 s, extension at 72°C for 1.5 min, and ending in a final extension step of 10 min. Archaeal 16S rRNA genes were amplified using the archaeal primer pair Ar109f and Ar912r (Grosskopf *et al.*, 1998; Lueders and Friedrich, 2000) as described above except that annealing was performed at 52°C and the extension was performed for 1 min.

Clone libraries of amplified 16S rRNA genes were generated using a cloning kit (TOPO TA Cloning Kit for Sequencing, Invitrogen, Carlsbad, CA) following the manufacturer's instructions. Clone libraries were constructed from samples collected on days 2 and 127 from both reactors. The libraries generated from the AMBR consisted of pooled amplicons from the five compartments obtained using the conditions described above.

Ninety-six clones from each bacterial clone library were screened initially by colony PCR (Gussow and Clackson, 1989) using vector-located sequencing primer sites (T3 and T7) to determine the presence of appropriately sized inserts. Thereafter, amplicons of the correct size (approximately 1400 bp) were digested with HaeIII and resolved on 1.5% NuSieve 3:1 agarose (Cambrex Bio Science, Rockland, ME). Plasmids from clones yielding restriction patterns (ARDRA patterns) that occurred more than once in each library were extracted using the alkaline lysis method (Sambrook and Russell, 2001) and used as template for bacterial PCR and T-RFLP analysis (see below). Of 46 clones selected for T-RF screening, 31 unique T-RF sizes were distinguished and compared with T-RF profiles from environmental samples. Clones with T-RF peaks corresponding to abundant peaks (defined as peaks constituting at least 20% of the cumulative peak heights in at least one sampling date) in environmental extracts were selected for subsequent sequencing. Eight complete sequences with unique T-RF sizes corresponding to abundant populations in the bioreactors during reactor operation were selected. Sequences of both strands were generated using an automated sequencer (ABI-Prism 3730, Applied Biosystems, Foster City, CA) operated by the W.M. Keck Center for Comparative and Functional Genomics at the University of Illinois at Urbana-Champaign Biotechnology Center (Urbana, IL). Sequence data were aligned and edited using MacVector software (Accelrys, San Diego, CA).

Archaeal clone libraries were analysed in a similar fashion as described above, except that only 48 clones from each library were analysed. Eleven unique restriction patterns (ARDRA types) generated three unique T-RF sizes. The identities of sequences representing each ARDRA and T-RF type were confirmed by sequencing (see above).

T-RFLP and data analysis

Polymerase chain reaction prior to T-RFLP used the same conditions as described above, except that the bacterial forward and the archaeal reverse primers were labelled at the 5′ end by 6-carboxyfluorescein (FAM). Amplicons from two replicate reaction mixtures were pooled using a PCR purification kit (QIAquick, Qiagen, Valencia, CA) and resuspended in 30 μl of the kit's elution buffer. Five microlitres of purified PCR product (approximately 600 ng) was digested at 37°C with 2.5 units of HaeIII (New England Biolabs, Beverly, MA) for 12 h followed by an enzyme inactivation step of 80°C for 20 min. The fluorescently labelled T-RFs were resolved with an automated sequencer (ABI-Prism 377, Applied Biosystems) using an internal size standard (TAMRA 2500, Applied Biosystems) operated by the W.M. Keck Center for Comparative and Functional Genomics at the University of Illinois at Urbana-Champaign Biotechnology Center. Terminal restriction fragment data were evaluated and converted to text format using Genescan 2.1 analysis software (Applied Biosystems).

We considered a minimum T-RF peak height of 50 fluorescent units to represent an operational taxonomic unit (OTU). Data sets exported from Genescan 2.1 were converted to spreadsheet format (Microsoft Excel, Microsoft, Redmond, WA) and normalized by obtaining the ratio of each peak height to the cumulative peak height.

The richness (S) of OTUs was obtained from the total number of distinct T-RFs in each profile. The Shannon–Weaver diversity index (H) (Atlas and Bartha, 1998) was calculated as follows: $H = -\Sigma\ (p_i)\ (\log\ p_i)$, where p is the proportion of an individual peak height relative to the cumulative peak height. All peaks (minimum height = 50 fluorescent units) representing fragment sizes less than undigested controls were included in determining S and H. The evenness (e) of T-RF peak heights was calculated as follows: $e = H/\log(S)$.

Similarities among T-RF profiles were evaluated using methods previously described (Blackwood *et al.*, 2003). Briefly, T-RF profiles were aligned manually in a spreadsheet program by considering peaks with sizes within 1 bp of each other as representing the same OTU. Due to current limitations of gel electrophoresis technology (Lerman and Frisch, 1982; Lumpkin *et al.*, 1985; Grossman *et al.*, 1992), and the possibility of contamination by the labelled primers, only fragment sizes between 30 and 536 bp were considered for similarity analysis. Euclidean distances between Hellinger-transformed (i.e. square root) relative peak height data (Legendre and Gallagher, 2001) were calculated and clustering by Ward's minimum variance method was performed using SAS statistical analysis software (SAS Institute, Cary, NC). In Ward's minimum variance method, the distance between clusters is represented by the ANOVA sum of squares of the two clusters added up for all the variables (transformed peak heights). Two clusters are merged during each generation to minimize the within cluster sum of squares. Branch

lengths between clusters are represented by the sum of squares divided by the total sum of squares, to yield the proportion of variance or the semi-partial r^2. Cluster analysis was performed on both replicates of each sample for every sampling period. In order to summarize the data, and to further illustrate the changing community structures, correspondence analysis was conducted on mean ($n = 2$) T-RF (relative peak heights) data from three sampling dates (days 2, 85 and 148). Correspondence analysis is a multivariate ordination method that allows taxa (T-RFs) and sites (compartments) to be plotted along axes that help explain most of the variation in the data. The analysis was performed using PAST, a paleontological statistics software (Hammer *et al.*, 2001) freely available on the Internet (http://folk.uio.no/ohammer/past/) or Excel© macros in Biplot (Lipkovich and Smith, 2002), which are also freely available (http://www.stat.vt.edu/facstaff/epsmith.html).

Phylogenetic analysis and accession numbers

Sequence alignments generated from MacVector (Accelrys, San Diego, CA) were converted to Phylip format and further analysed using Phylip 3.6 (Felsenstein, 2002). The phylogenetic tree in Fig. 4 was generated using the maximum likelihood algorithm, DNAML. Tree topology was confirmed by comparing neighbour joining trees using Jukes and Cantor and Kimura 2-parameter distance methods in Phylip 3.6. Robustness was tested by bootstrap resampling from 100 maximum likelihood analyses. Sequences generated in this study are available from GenBank, EMBL and the DNA Databank of Japan under accession numbers AY648563–AY648570.

Acknowledgements

Funding was provided by the Illinois Department of Natural Resources (Contract No. HWR01168) and by the Water-CAMPWS US National Science Foundation (Grant No. 0120978).

References

Angenent, L.T., and Sung, S.W. (2001) Development of anaerobic migrating blanket reactor (AMBR), a novel anaerobic treatment system. *Water Res* **35:** 1739–1747.

Angenent, L.T., Zheng, D.D., Sung, S.H., and Raskin, L. (2002a) Microbial community structure and activity in a compartmentalized, anaerobic bioreactor. *Water Environ Res* **74:** 450–461.

Angenent, L.T., Abel, S.J., and Sung, S. (2002b) Effect of an organic shock load on the stability of an anaerobic migrating blanket reactor. *J Environ Eng* **128:** 1109–1120.

Angenent, L.T., Sung, S.W., and Raskin, L. (2002c) Methanogenic population dynamics during startup of a full-scale anaerobic sequencing batch reactor treating swine waste. *Water Res* **36:** 4648–4654.

Annachhatre, A.P., and Suktrakoolvait, S. (2001) Biological sulfate reduction using molasses as a carbon source. *Water Environ Res* **73:** 118–126.

Atlas, R.M., and Bartha, R. (1998) *Microbial Ecology: Fundamentals and Applications*. Menlo Park, CA, USA: Benjamin/Cummings Science Publishing.

Balk, M., Weijma, J., and Stams, A. (2002) *Thermotoga lettingae* sp. nov., a novel thermophilic, methanol-degrading bacterium isolated from a thermophilic anaerobic reactor. *Int J Syst Evol Microbiol* **52:** 1361–1368.

Barber, W.P., and Stuckey, D.C. (1999) The use of the anaerobic baffled reactor (ABR) for wastewater treatment: a review. *Water Res* **33:** 1559–1578.

Blackwood, C.B., Marsh, T., Kim, S.H., and Paul, E.A. (2003) Terminal restriction fragment length polymorphism data analysis for quantitative comparison of microbial communities. *Appl Environ Microbiol* **69:** 926–932.

Choi, E., and Rim, J.M. (1991) Competition and inhibition of sulfate reducers and methane producers in anaerobic treatment. *Water Sci Technol* **23:** 1259–1264.

Colleran, E., Finnegan, S., and Lens, P. (1995) Anaerobic treatment of sulfate-containing waste streams. *Antonie Van Leeuwenhoek* **67:** 29–46.

Daugherty, B.J. (2002) Anaerobic treatment of high sulfate waste streams to allow for the subsequent recovery of sulfur. MSc Thesis. Urbana, IL: University of Illinois at Urbana-Champaign.

Felsenstein, J. (2002) *Phylogeny Inference Package*, Version 3.6a3. Distributed by the Author. Seattle, WA: Department of Genome Sciences, University of Washington.

Franklin, R.J. (2001) Full-scale experiences with anaerobic treatment of industrial wastewater. *Water Sci Technol* **44:** 1–6.

Godon, J.J., Zumstein, E., Dabert, P., Habouzit, F., and Moletta, R. (1997) Molecular microbial diversity of an anaerobic digestor as determined by small-subunit rDNA sequence analysis. *Appl Environ Microbiol* **63:** 2802–2813.

Greenberg, A.E., Clesceri, L.S., and Eaton, A.D. (1992) *Standard Methods for the Examination of Water and Wastewater.* Washington, DC, USA: APHA, AWWA and WEF.

Griffin, M.E., McMahon, K.D., Mackie, R.I., and Raskin, L. (1998) Methanogenic population dynamics during start-up of anaerobic digesters treating municipal solid waste and biosolids. *Biotechnol Bioeng* **57:** 342–355.

Grosskopf, R., Janssen, P.H., and Liesack, W. (1998) Diversity and structure of the methanogenic community in anoxic rice paddy soil microcosms as examined by cultivation and direct 16S rRNA gene sequence retrieval. *Appl Environ Microbiol* **64:** 960–969.

Grossman, P.D., Menchen, S., and Hershey, D. (1992) Quantitative-analysis of DNA-sequencing electrophoresis. *Genet Anal Tech Appl* **9:** 9–16.

Gussow, D., and Clackson, T. (1989) Direct clone characterization from plaques and colonies by the polymerase chain-reaction. *Nucleic Acids Res* **17:** 4000–4000.

Hammer, O., Harper, D.A.T., and Ryan, P.D. (2001) PAST: paleontological statistics software package for education and data analysis. *Palaeontologia Electronica* **4:** 9p

Hansen, K.H., Ahring, B.K., and Raskin, L. (1999) Quantification of syntrophic fatty acid-beta-oxidizing bacteria in a mesophilic biogas reactor by oligonucleotide probe hybridization. *Appl Environ Microbiol* **65:** 4767–4774.

Harada, H., Uemura, S., and Momonoi, K. (1994) Interaction between sulfate-reducing bacteria and methane-producing bacteria in Uasb reactors fed with low strength wastes containing different levels of sulfate. *Water Res* **28:** 355–367.

Lane, D.J. (1991) 16S/23S rRNA sequencing. In *Nucleic Acid Techniques in Bacterial Systematics*. Stackebrandt, E., and Goodfellow, M. (eds). Chichester, UK: John Wiley & Sons, pp. 115–175.

Legendre, P., and Gallagher, E.D. (2001) Ecologically meaningful transformations for ordination of species data. *Oecologia* **129:** 271–280.

Lens, P.N.L., Visser, A., Janssen, A.J.H., Pol, L.W.H., and Lettinga, G. (1998) Biotechnological treatment of sulfate-rich wastewaters. *Crit Rev Environ Sci Technol* **28:** 41–88.

Lerman, L.S., and Frisch, H.L. (1982) Why does the electrophoretic mobility of DNA in gels vary with the length of the molecule. *Biopolymers* **21:** 995–997.

Lettinga, G., van Velsen, A.F.M., Hobma, S.W., de Zeeuw, W., and Klapwijk, A. (1980) Use of the upflow sludge blanket (USB) reactor concept for biological wastewater treatment, especially for anaerobic treatment. *Biotechnol Bioeng* **22:** 699–734.

Lipkovich, I.A., and Smith, E.P. (2002) Biplot and singular value decomposition macros for Excel. *J Stat Software* **7:** 15.

Lueders, T., and Friedrich, M. (2000) Archaeal population dynamics during sequential reduction processes in rice field soil. *Appl Environ Microbiol* **66:** 2732–2742.

Lumpkin, O.J., Dejardin, P., and Zimm, B.H. (1985) Theory of gel-electrophoresis of DNA. *Biopolymers* **24:** 1573–1593.

McMahon, K.D., Stroot, P.G., Mackie, R.I., and Raskin, L. (2001) Anaerobic codigestion of municipal solid waste and biosolids under various mixing conditions – II: Microbial population dynamics. *Water Res* **35:** 1817–1827.

McMahon, K.D., Zheng, D., Stams, A.J., Mackie, R.I., and Raskin, L. (2004) Microbial population dynamics during start-up and overload conditions of anaerobic digesters treating municipal solid waste and sewage sludge. *Biotechnol Bioeng* **87:** 823–834.

Mizuno, O., Li, Y.Y., and Noike, T. (1994) Effects of sulfate concentration and sludge retention time on the interaction between methane production and sulfate reduction for butyrate. *Water Sci Technol* **30:** 45–54.

Raskin, L., Poulsen, L.K., Noguera, D.R., Rittmann, B.E., and Stahl, D.A. (1994) Quantification of methanogenic groups in anaerobic biological reactors by oligonucleotide probe hybridization. *Appl Environ Microbiology* **60:** 1241–1248.

Ravot, G., Ollivier, B., Magot, M., Patel, B., Crolet, J., Fardeau, M., and Garcia, J. (1995) Thiosulfate reduction, an important physiological feature shared by members of the order thermotogales. *Appl Environ Microbiol* **61:** 2053–2055.

Sambrook, J., and Russell, D.W. (2001) *Molecular Cloning: A Laboratory Manual*. Cold Spring Harbor, NY, USA: Cold Spring Harbor Laboratory Press.

Sekiguchi, Y., Kamagata, Y., Syutsubo, K., Ohashi, A., Harada, H., and Nakamura, K. (1998) Phylogenetic diversity of mesophilic and thermophilic granular sludges determined by 16S rRNA gene analysis. *Microbiology* **144:** 2655–2665.

Speece, R.E. (1996) *Anaerobic Biotechnology for Industrial Wastewaters*. Nashville, TN, USA: Archae Press.

Stetter, K.O., Fiala, G., Huber, G., Huber, R., and Segerer, A. (1990) Hyperthermophilic microorganisms. *FEMS Microbiol Rev* **75:** 117–124.

Winker, S., and Woese, C.R. (1991) A definition of the domains Archaea, Bacteria and Eukarya in terms of small subunit ribosomal RNA characteristics. *Syst Appl Microbiol* **13:** 161–165.

Yamaguchi, T., Harada, H., Hisano, T., Yamazaki, S., and Tseng, I.-C. (1999) Process behavior of UASB reactor treating a wastewater containing high strength sulfate. *Water Res* **33:** 3182–3190.

Zehnder, A.J.B., Huser, B.A., Brock, T.D., and Wuhrman, K. (1980) Characterization of an acetate-decarboxylating, non-hydrogen-oxidizing methane bacteria. *Arch Microbiol* **124:** 1–11.

Zheng, D., Angenent, L.T., and Raskin, L. (2006) Monitoring granule formation in anaerobic upflow bioreactors using oligonucleotide hybridization probes. *Biotechnol Bioeng* **94:** 458–472.

